

We are IntechOpen, the world's leading publisher of Open Access books Built by scientists, for scientists

6,700

Open access books available

180,000

International authors and editors

195M

Downloads

Our authors are among the

154

Countries delivered to

TOP 1%

most cited scientists

12.2%

Contributors from top 500 universities



WEB OF SCIENCE™

Selection of our books indexed in the Book Citation Index
in Web of Science™ Core Collection (BKCI)

Interested in publishing with us?
Contact book.department@intechopen.com

Numbers displayed above are based on latest data collected.
For more information visit www.intechopen.com



Chapter

Mercury Emission from Prescribed Open Grassland Burning in the Aso Region, Japan

*Satoshi Irei, Satoshi Kameyama, Hiroto Shimazaki,
Asahi Sakuma and Seiichiro Yonemura*

Abstract

In every Spring, prescribed grassland burning, so-called Noyaki in Japanese, has been conducted for over a 1000 years by local residents in the Aso region, Japan, for the purpose of grassland conservation because Noyaki prevents invasion of woody plants in the grassland and helps the growth of grasses, which were an important resource of primary industry for roofing materials of houses and livestock feed. Meanwhile, biomass burning is known to be one of the most significant sources of airborne substances including mercury. Taking advantage of the characteristics and resources of the place we live in, we here describe our on-going study for the emission of gaseous mercury from the traditional Noyaki in the Aso region and other grasslands of western Japan. During Noyaki, we sampled and measured gaseous mercury from the Noyaki plumes to better understand mercury emissions and cycles in the local environment. Results showed, on average, 3.8 times higher atmospheric mercury concentrations, demonstrating the emission of gaseous mercury from the Noyaki. The possible origins, novel information the results inferred, and future research direction are discussed in this chapter.

Keywords: Minamata convention on mercury, gaseous mercury, biomass burning, plant uptake, dry deposition, wet deposition

1. Introduction

1.1 Prescribed open grassland burning in the Aso region for the conservation of grassland

The country of Japan consists of 14,125 islands, is located at the longitude between 153°59'12" and 122°55'57" and the latitude between 20°25'31" and 45°33'26", and has the total area of 377, 974.17 km² (**Figure 1a**) [1]. Approximately 126 million people reside in this country [2]. Depending on the region, the climate is divided into sub-tropical, temperate, or boreal and the temperate predominantly covers most of the land. Japan is a green country; forests and grassland account for 66 and 5% of the whole land [3, 4]. The largest grassland in Japan is located in the Aso region, Kumamoto Prefecture.

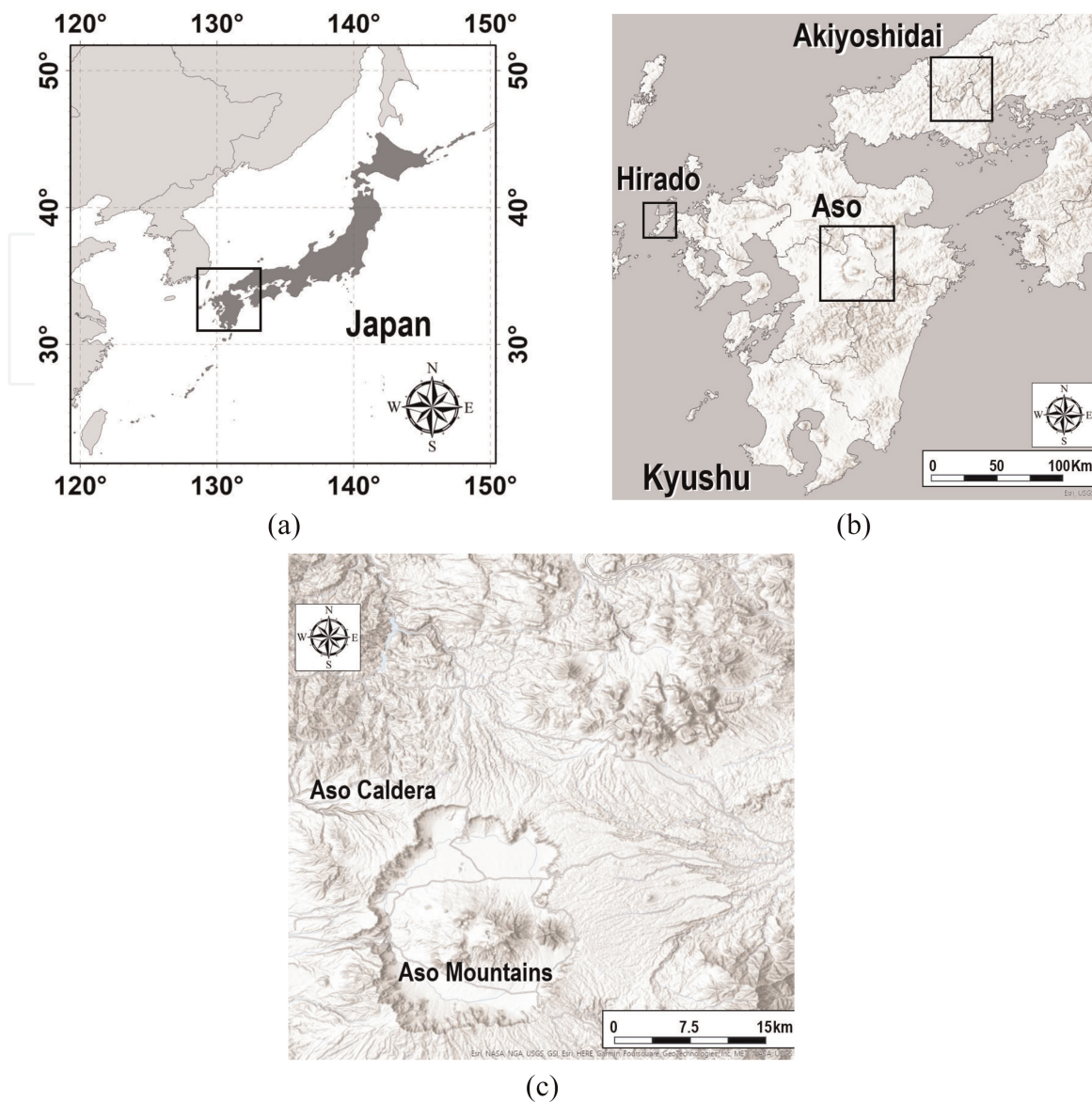


Figure 1. (a) Map of Japan, (b) Kyushu Mainland, and (c) Aso Region. Map images are from the Elevation World Hillshade (courtesy to the ESRI base map, <https://doc.arcgis.com/en/data-appliance/2022/maps/world-hillshade.htm>).

Aso is a regional name and it is located nearly in the center of Kyushu Island in western Japan (**Figure 1b**). Geographically, this region consists of a large caldera (463 km²) with the surrounding area (**Figure 1c**). The altitude is between 400 and 800 m, and the average temperature throughout the year is 13°C approximately [5]. Active volcanoes located in the center of the caldera, “the Aso five mountains”, are the landmark of this region. With respect to local governments, the Aso region consists of seven municipalities: Aso city, Oguni town, Minami Oguni town, Takamori town, Ubuyama village, Minami Aso village, Nishihara village. Agriculture, pasture, and tourism are the major industries in these municipals, and the latter two use grasslands. The landscape of the grassland contributes to the local economy. Approximately 1,850,000 tourists in 2018 and 829,000 tourists visited and stayed in the Aso region [6, 7]. This accounts for approximately 23% of tourist visits of Kumamoto Prefecture. Highland breeze in the grassland attracts visitors from all over Japan and overseas.

The grasslands in the Aso region and other local areas such as Hirado in Nagasaki Prefecture and the Akiyoshi-dai plateau in Yamaguchi Prefecture are burnt every Spring (e.g., **Figure 2a** and **b**) after the annual grass dies and dried during the late Fall (**Figure 3**).



(a)



(b)

Figure 2.
(a and b) Photograph of Noyaki in Aso.



Figure 3.
Photograph of the Aso grassland before Noyaki.

The grassland burning is called “Noyaki” or “Yamayaki” in Japanese (referred to as Noyaki hereafter). According to a scientific study, Noyaki in Aso has been conducted since 10,000 years ago [8]. The purpose of Noyaki in the ancient era was to have open sight for hunting wild animals, but now it has shifted to the prevention of wild forestation of the unused lands, pest control, and reset of annual habitat plants [8, 9]. With this background, there is no doubt that people love Noyaki and it is a symbol of Spring’s coming.

1.2 Plant communities in the Aso grassland

The grasslands of the Aso region in Kyushu, Japan, exist both inside and outside of the Aso-Kuju National Park, which covers an area of 72,680 ha [10]. The area of grassland dominated by native species such as *Miscanthus* (*Miscanthus sinensis*) and *Nezasa* (*Pleiolblastus chino var. viridis*) within the national park, covering approximately 15,000 ha, approximately 43% of whole grassland in the Aso region [11]. In the grassland, controlled or prescribed burning is conducted as a traditional event every March. This artificial burning event has a significant impact on the regeneration of grassland vegetation and the dominance of certain species. The dominant plant species in the burned grassland include the following [12, 13]: Herbaceous plants of *Miscanthus* (*Miscanthus sinensis*), bamboo grass (*Pleiolblastus chino var. viridis*), Eulalia grass (*Miscanthus transmorrisonensis*), silver grass (*Miscanthus sacchariflorus*), pampas grass (*Miscanthus floridulus*), Japanese yamayuzu (*Fallopia japonica*), Japanese ladybell (*Adenophora triphylla*), bracken fern (*Pteridium aquilinum*); Shrubs of willows (*Salix spp.*), oaks (*Quercus spp.*), sourberries (*Viburnum spp.*), mountain azaleas (*Rhododendron brachycarpum*), painted ferns (*Athyrium niponicum*),

hydrangeas (*Hydrangea spp.*), honeysuckles (*Lonicera spp.*), and others. Furthermore, the following plants, which invaded during the time when the mainlands of Japan, Kyushu, and Shikoku islands were connected to the Asian continent, remain as endemic species: “Continental relics”: field chickweed (*Stellaria matsudae*), false hellebore (*Veratrum nigrum*), daylily (*Heemerocallis citrina*); “Boreal plants”: herbaceous saxifrage (*Saxifraga stolonifera*), golden-rayed lily (*Lilium auratum*), Bistort (*Bistorta officinalis Delarbre subsp. japonica*), lilies (*Lilium spp.*).

1.3 Mercury emission from grassland burning

Crutzen et al. [14] reported the significance of biomass burning as a source of airborne substances in the global atmosphere. Since then extensive emission studies have been done on this subject in fields (*e.g.*, [15–31]), in laboratories (*e.g.*, [32–40]), by satellites (*e.g.*, [40]), and by modeling [41–45]. Published results have also been reviewed (*e.g.*, [46–49]).

Veiga et al. [50] reported indirect observations of gaseous mercury emissions from biomass burning for the first time. Since then gaseous mercury from biomass burning has also been studied in North America [37, 51–53], Africa [54], Europe and Russian Federation [55], South America [56], long-range transport [57–59], and laboratory [38, 40]. To date, it has been reported that biomass burning accounts for ~8% of global mercury emissions to the atmosphere [60]. To the best of our knowledge, the emission of mercury from Noyaki in Japan was reported for the first time by Irei [61, 62]. Its stable mercury isotopic compositions were also reported for the first time worldwide. Even though the emission size may not be as large as wildfires overseas, there is no information available for Noyaki to that date.

Plants are known to uptake mercury from the ground and ambient air (*e.g.*, [63–82]). Sawgrass, a dominant plant species found in the Aso region, is also not an exception. Sawgrass in Florida, relative plant species of Japanese sawgrass, inhales gaseous mercury from the air and fixes it in its own body [83]. Thus, there is no surprise even if Japanese Noyaki emits gaseous mercury to the atmosphere.

The Japanese Ministry of Environment recently updated the domestic emission inventory of mercury for the fiscal year of 2020 (**Figure 4**) [84], showing that ~87% of mercury, out of 10.7 tons of annual mercury emissions, originates from anthropogenic sources. Only volcanic emissions, accounting for ~13%, are the source other than anthropogenic sources. In order to better the mercury cycle in the natural environment, we should not miss any significant source, and Noyaki is one of the veiled domestic emission sources. How much of gaseous mercury was emitted during Noyaki? From where did the emitted mercury come from? Finding answers to these open questions will make our mercury cycle studies progress.

In general, the total emission (TE, g) of chemical species of interest from biomass burning can be estimated using a common mass balance approach.

$$TE = FL \times BA \times CE \times EF \quad (1)$$

where a fuel load or FL, also used to be referred to as a “biomass density”, is a dried mass of biomass per unit area (typically in kg m^{-2}), burned area or BA is the total area burnt (m^2), combustion efficiency or CE is the fraction of converted biomass carbon to airborne carbonaceous products, such as carbon dioxide (CO_2), and an emission factor or EF is the quantity of substance of interest emitted per kg of biomass burnt (g kg^{-1}) [18, 47, 51, 60, 85]. FL can be estimated according to the information on the biomass

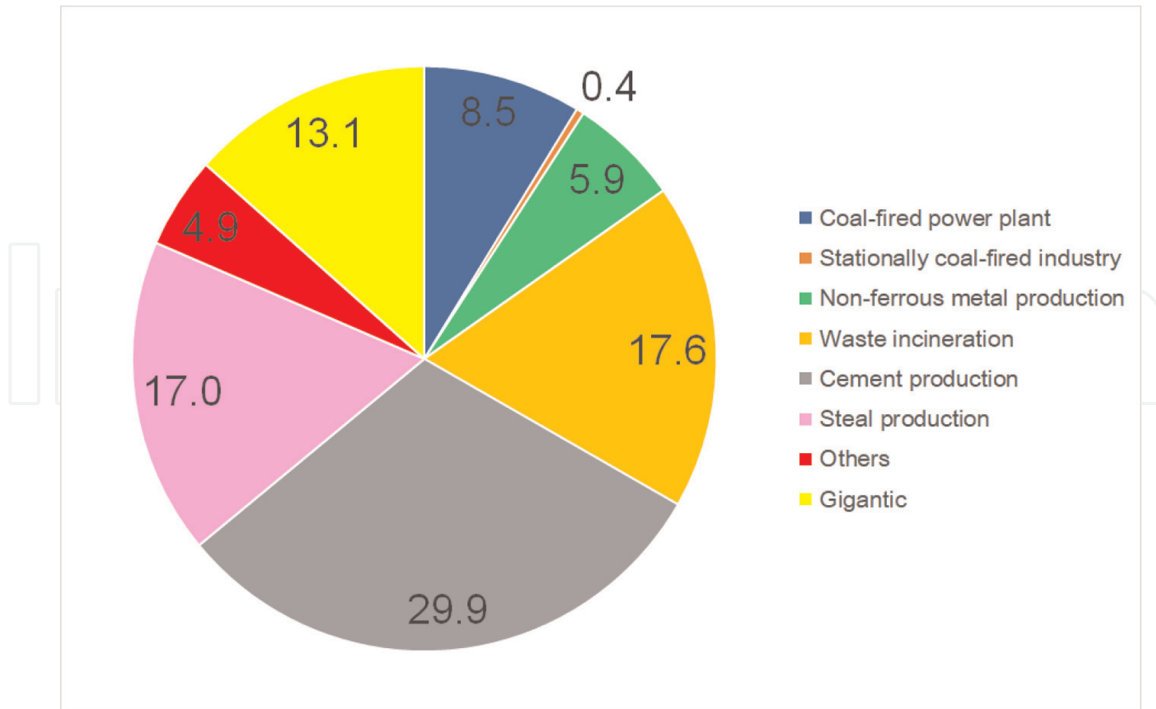


Figure 4. Domestic Hg emission inventory. The chart was produced according to the information that the Japanese Ministry of Environment has published for the year of 2020 (website). The values are relative to the total domestic Hg emission, 10.7 tons y^{-1} .

density map [41], but it can also be measured directly (e.g., [24–26, 60]). For a large area, FL is highly uncertain [42]. BA is primarily achieved using remote sensing technology through two methods [86]: The approach involving calculation of the extent of the burned area through the comparison of two images taken before and after the fire [87, 88] and the approach involving time-series analysis of regularly captured satellite images from the real-time monitoring of the fire [89] using the MODIS satellite (<https://modis.gsfc.nasa.gov/data/dataproduct/mod14.php>). A CE is hard to know in a real fire, but a modified CE (MCE), the excess concentration (denoted as Δ hereafter, which is the concentration during Noyaki subtracted by the background concentration) ratio of CO_2 to the sum of excess concentrations of carbon monoxide (CO) and CO_2 ($\Delta\text{CO} + \Delta\text{CO}_2$), has been used as an alternate index of CE [18, 90]. An EF for a substance of interest is a key parameter depending on the types and moisture content of the fuel and burning conditions (smoldering and flaming fires). Of the parameters and variable in Eq. (1), EFs have been most intensively discussed in biomass-burning emission studies (e.g., [46]). An EF can be further broken down to as follows [18, 46]:

$$\text{EF} = \text{ER} \times \frac{\text{MW}_i}{12} \times \text{CC} \times 1000 \quad (2)$$

ER is an excess mole concentration ratio of the targeted substance to the sum of the excess carbon mole concentrations of carbonaceous (reference) substances, which are measured in field studies, MW_i is the molecular weight of substance of interest ($200.59 \text{ g mol}^{-1}$ in the case of mercury), 12 is the atomic mass of carbon, and CC is the carbon content of fuel, which is often assumed as 0.5 [18, 36], and 1000 is a conversion factor for the product in g base to kg base. It should be noted that the sum of the excess concentrations of carbonaceous species is often approximated as the sum of ΔCO and ΔCO_2 or the excess mole concentration of CO_2 divided by MCE.

1.4 Sampling and measurement

In the Aso region, there are a number of stock farms and they possess own grasslands. In every Spring they burn the grasslands to restore the perennial plants. Thus, occurrences of prescribed fires are spotted over the region. Approximately 160 km² of the Aso grassland is burnt in total every Spring [91].

Field sampling and measurements for chemical substances emitted from Noyaki can be conducted by either airborne or on the ground. The former method (*i.e.*, use of aircraft) is often chosen in biomass burning studies overseas because open biomass burnings, mostly wildfires, are large and data gained during flights over plumes can represent the emission [46]. It is also because airborne sampling and measurements are more safely conducted. However, the high cost, limited accessibility, fast moving speed, etc. of manned aircraft sampling and measurements are overpowered in the Japanese Noyaki studies where only one or few km² of grassland is burnt at each stock farm. Meanwhile, ground-based sampling and measurements can be done at fixed measurement stations and/or on ground vehicles. The advantages of ground-based measurements are that instruments and measuring devices can be set more easily and quickly, compared to aircraft measurements. Relatively low cost of use of cars is another advantage. However, the success of ground-based measurements strongly relies on the weather conditions, such as wind speed and directions, proximity to the fires and plumes, landscapes of grasslands, paved roads one can drive vehicles on, etc. Depending on how quickly fire spreads, safety is another factor that one must consider. In our field studies, we have chosen ground-based sampling and measurements using vehicles.

In biomass burning studies, measurements of CO and CO₂ are the base because the major products of biomass burning are CO₂ and CO, accounting for more than 95% of products in general, and their ratio often indicates burning conditions, such as smoldering and flaming. CO₂ and CO are also contained in background air, therefore, their excess concentrations from their background level need to be checked for the evaluation of burning conditions.

Gaseous mercury concentrations can be measured either by automated mercury analyzers or the combination of conventional amalgam trap sampling and its offline analysis using a cold-vapor atomic fluorescent or absorbance spectrometer.

For stable mercury isotope analysis, nano gram order of total gaseous mercury (TGM) needs to be collected. This collection can be done through either chemical traps [92], multiple commercially available gold amalgam sampling tubes [80, 93], or large volume gold amalgam sampling tubes, namely BAuTs [62]. Collected TGM was then converted to gaseous elemental mercury (GEM) by heating, and the converted GEM is oxidized to Hg²⁺ and captured in sulfuric acid/permanganate mixture or reversed aqua regia mixture. Prepared sample solutions were then analyzed by a multi-collector inductively coupled plasma mass spectrometer or MC-ICP-MS.

1.5 Potential of Noyaki studies in western Japan

Since the start of our Noyaki emission studies in 2019, solid evidence of mercury emission has been confirmed [61, 62]. The papers also report the similarly fractionated $\delta^x\text{Hg}$ values of the excess TGM to the fractionated $\delta^x\text{Hg}$ values of mercury found in plant species reported by others, implying that the excess TGM was likely supplied from the grassland plant. The pilot studies above gave us an overview of what was happening during the Noyaki events and raised some intriguing open questions: How

much was TGM produced and emitted to the atmosphere from Noyaki in this region? What was the origin of TGM emitted from Noyaki?

The first question is the primary one that anyone will have. This estimation has not ever been done, thus, the source has not been included yet in the domestic mercury emission inventories of gaseous mercury that the Ministry of Environment Japan has ever reported. Under the current circumstance that a number of nations implement the regulation on man-made mercury use, namely the Minamata Convention on Mercury, this evaluation is worthwhile and contributes to update the mercury budget. It is also interesting how variable “the annual routine emissions” are. Such information is new and can be gained only from the prescribed burning conducted routinely. The information can be extended to the fate of atmospheric mercury, which can be applicable not only to the local environment but global one as well.

The second question delves into the mercury cycle in detail. Identifying the origin (s) will help us to better understand phenomena occurring on mercury in the natural environment, which contributes to the intellectual and novel input into our current understanding of mercury cycle.

2. Methodology

2.1 Estimation of burnt area

In the following manner, we conducted the process of satellite image analysis. First, we downloaded Landsat-8 surface reflectance and surface temperature products (path = 112, row = 037) observed on April 9, 2023, from the United States Geological Survey Earth Explorer website (<https://earthexplorer.usgs.gov/>). For the purpose of creation of a spatial distribution map of prescribed burns, we adopted a supervised classification approach. In this classification method, we curated ground reference data for two classification categories: “burned” and “unburned.” In the next step, we selected three vegetation groups: “pastureland,” “*Miscanthus sinensis* (including *Pleioblastus chino* var. *viridis*) stand”, and “*Miscanthus sinensis* (excluding *Pleioblastus chino* var. *viridis*) stand” using a 1:25,000 scale existing vegetation map. To reduce spatial bias in the ground reference data, we determined 130 reference points from each group. For the three selected vegetation groups (130 ground reference data points each × 3), we randomly allocated “training data (100)” and “validation data (30)” for each vegetation group. We adopted the Random Forest algorithm, a type of machine learning algorithm with a proven track record in land use and land cover classification using satellite imagery. This algorithm was executed using the random Forest package (version 4.7.1.1) in R (version 4.2.1). For the classification results of the controlled burns’ spatial distribution map, we evaluated the accuracy with overall accuracy and a Kappa coefficient.

2.2 Fuel loads and emission factor

For wildfire studies, fuel load information can be gained from estimation based on CO and CO₂ measurements under the assumption that the fuel burned contains 50% of carbon content in weight (*e.g.*, [18, 36]) or from the actual analysis of habitat plants in the field [73]. The former is a top-down method and practical for cases where sampling biomass representing the habitat plants in the burned area is difficult (*e.g.*, forests with a large diversity of plant species). In contrast, the latter, a bottom-up method of actual



(a)



(b)

Figure 5. Photograph of example of sampling aboveground grass in a 1×1 m quadrat: (a) before the grass was reaped, and (b) after the grass was reaped.

measurements of biomass, is ideal. For the Aso grassland, this ideal case can be applied because the composition of plant species is simple; only two plant species, *Miscanthus sinensis* and *Pleioblastus chino var. viridis*, predominantly occupy the grassland burned. This makes the retrieval of aboveground fuel loads and chemical contents of the biomass pool feasible.

Fuel load, the mass of biomass per unit area, was obtained experimentally in the Aso grassland study. In the grassland, a 1×1 m square quadrat was defined using plastic rods, then the plants and litters within the quadrat were sampled (Figure 5). The plant samples were then brought to the laboratory, and dried in the air-conditioned room (24° C and 24% for temperature and humidity, respectively) until the masses were stabilized. Their masses and chemical contents were then measured. If combustion completeness, $CE = 1$, is given, an EF for a substance of interest will be equivalent to the content in the biomass, thus, the EF will be easily gained from this bottom-up approach.

2.3 Sampling and measurement of airborne chemical species

In our emission study in Aso, sampling and measurements for airborne chemical species were conducted in a vehicle. In-situ measurements for CO and CO₂ were made by a CO analyzer (Model 48C, Thermo Fisher Scientific.) and a CO₂ analyzer (LI-810, LI-COR Corp., Lincoln, NB, U.S.A.). For TGM measurements, plume gas was drawn through a gold-coated sand trap (N-160, Nippon Instruments Corp., Osaka, Japan) at the rate of 0.5 L min^{-1} using a mini-air pump (MP-W5P, Shibata Scientific Technology Ltd., Souka, Japan), and the tube samples were brought to the laboratory and analyzed for TGM by cold-vapor atomic fluorescent spectroscopy (CV-AFS, Nippon Instruments Corp.). TGM for stable mercury isotope analysis was captured through a BAuT sampling tube [61, 62] at the flow rate of 80 L min^{-1} . After the sampling, the BAuT tube was brought to the laboratory, then the TGM captured was converted to oxidized mercury (II) in 40% reversed aqua regia solution. The prepared solution samples were then analyzed by an MC-ICP-MS (Neptune Plus, Thermo Fisher Scientific GmbH, Bremen, Germany) for the isotopic composition.

$$\delta^x\text{Hg}(\text{‰}) = \left[\frac{\left(\frac{{}^x\text{Hg}}{198\text{Hg}} \right)_{\text{sample}}}{\left(\frac{{}^x\text{Hg}}{198\text{Hg}} \right)_{3133}} - 1 \right] \times 1000 \quad (3)$$

where x stands for the stable mercury isotope with mass x, and the bracketed isotope ratios with subscripts “sample” and “3133” indicate the stable mercury isotope ratios of mass x relative to the mass 198 for the sample and SRM 3133 (NIST), respectively.

Either a Teflon-coated glass fiber filter (Pallflex, Emfab, Pall Corp., Port Washington, NY, U.S.A.) or quartz fiber filter (Pallflex, Tissuequartz, Pall Corp.) installed in filter holder (Innovation NILU AS, Kjeller, Norway) or capsule filter (Balston, Parker Hannifin Corp., Cleveland, IL, U.S.A.) was attached to all the inlets for sampling and measurements described above.

Instruments and devices referred above were loaded to a vehicle, together with batteries for their power supplies, then plumes from Noyaki were chased. When the car was drove into plumes the car was stopped in the plumes and the engine was stopped until the plume is gone. The sampling and measurements were continued until the Noyaki of the day there ended.

3. Results and discussion

3.1 Burned area

There have been previous efforts that estimate the extent of BA in the Aso region using satellite imagery [94]. However, the estimates were based on the conventional maximum likelihood method and the reliability of the estimates was not evaluated. In our study, we employed the Random Forest algorithm, which is a machine learning method with better classification performance than the maximum likelihood method, and then evaluated the reliability of classification results in terms of overall accuracy and Kappa coefficient. The image analysis results (spatial distribution map of prescribed burns) were very accurate, with an overall accuracy of 0.972 and a Kappa coefficient of 0.944. This analysis demonstrated the potential and practical utility of high-precision spatial distribution estimation for prescribed burn monitoring using satellite imagery. Within the boundaries of individual pasturelands, areas that have undergone prescribed burns and those that have not were intermixed. The obtained data were used for more precise determination of the burnt area on more fine scale, and currently, boundaries are under the cross check. For future work, estimating burned biomass in prescribed burn monitoring, the capability of satellite image analysis covering extensive areas (enabling spatial distribution understanding) will be highly effective and essential (**Figure 6**).

3.2 Measurements

3.2.1 Aboveground fuel loads

Aboveground fuel loads we found in the Aso region are listed in **Table 1**. The table also shows fractions of two major habitat plant species, *Miscanthus sinensis* and *Pleioblastus chino var. viridis*. Results showed that the fuel loads were highly variable, from 0.6 to 1.58 kg m⁻². The compositions at most of the locations, except Minamioguni 1, were split by the two plant species. Minamioguni 1 was surrounded by trees, and, therefore, the most contributing, biofuel there was litter, which was included as other. Compared to the fuel loads reported to date, such as for African savanna (0.36–0.48 kg m⁻² [25], 0.20–2.5 kg m⁻² [95]), Austrarian savanna (0.56 kg m⁻² [24], 0.11–0.74 kg m⁻² [95]), North American meadow (0.4 kg m⁻², [52]), and central and south American savanna (0.30–1.38 kg m⁻² [95]), our observations were in compatible level.

3.2.2 TGM concentration

Observed atmospheric concentrations of TGM in the background air and Noyaki plumes were on average (\pm SD) 1.4 \pm 0.5 and 5.2 \pm 3.6 ng m⁻³, respectively. TGM concentrations varied substantially (**Figure 7**) and the variation was attributed to the proximity to the fire. With consideration of this atmospheric dilution, we are now confident that Noyaki indeed emits TGM into the atmosphere. As stated earlier, this emission has not been included in the Japanese domestic emission inventory that the Ministry of Environment Japan published, therefore, the emission source needs to be evaluated for a better understanding of the mercury cycle in the natural environment.

3.2.3 CO and CO₂ measurements

We defined the background concentrations of CO and CO₂ as 0 ppmv and 422 ppmv, respectively. Therefore, for our data, the subtraction of these concentrations

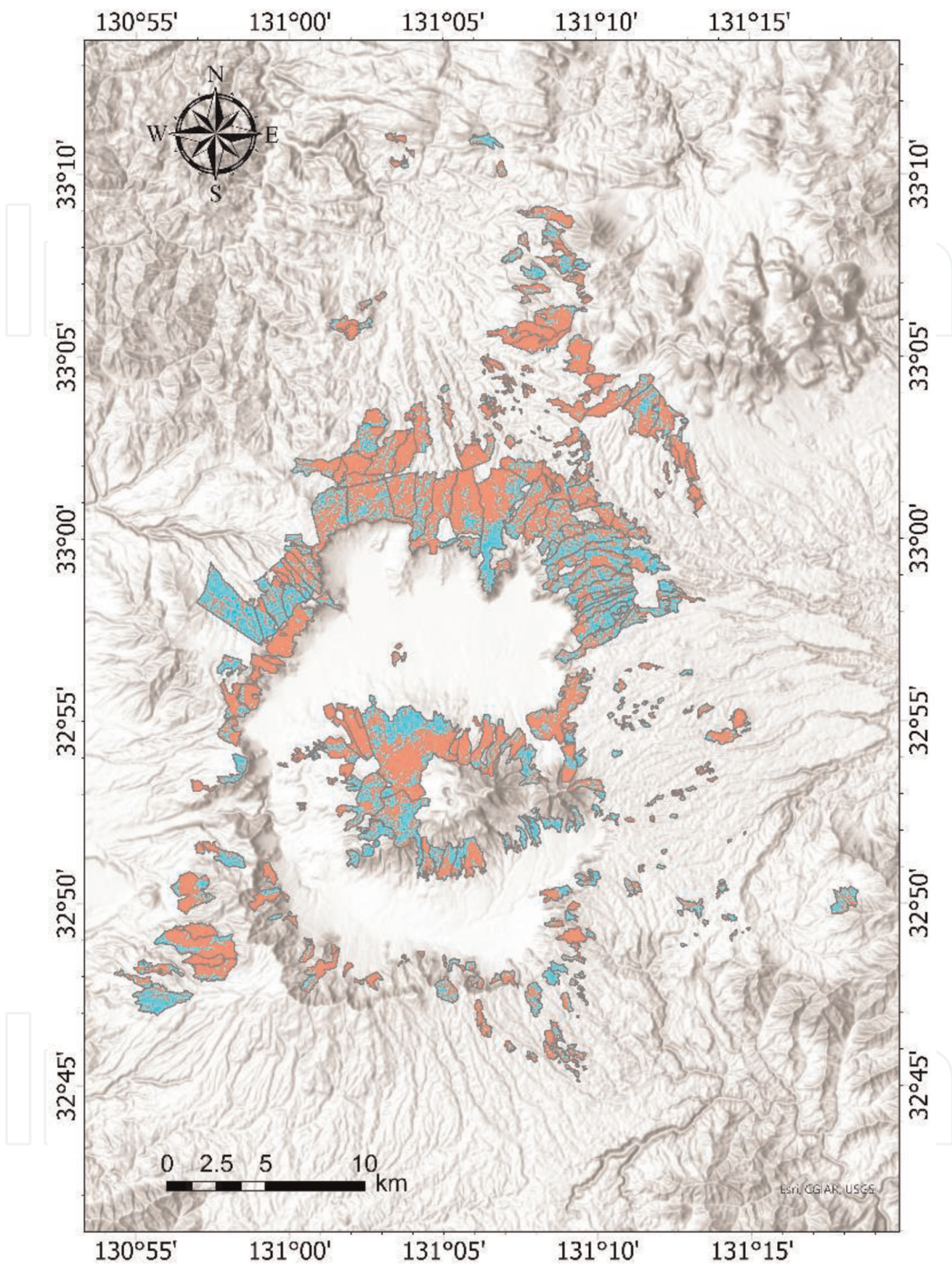


Figure 6. Overlaid images of a landscape map and burned (red) and unburned (light green) grasslands of the Aso region identified from the satellite images. Sources of the landscape map: World Hillshade, Esri, Airbus DS, USGS, NGA, NASA, CGIAR, N Robinson, NCEAS, NLS, OS, NMA, Geodatastyrelsen, Rijkswaterstaat, GSA, Geoland, FEMA, Intermap, and the GIS user community.

was applied due to their mixing ratios observed in the background air. Using the results obtained from the field study at the Akiyoshidai National Park, we show the overview of this research project.

Sampling location	Fuel load (kg m ⁻²)	<i>Miscanthus sinensis</i> (%)	<i>Pleiblastus chino var. viridis</i> (%)	Other (%)
Hirado	1.09	n.a.	n.a.	n.a.
Nishihara	1.58	n.a.	n.a.	n.a.
Minamioguni 1	0.60	29.5	31.5	39.0
Minamioguni 2	0.74	67.6	22.9	9.5
Kamitajiri	0.96	27.4	71.6	0.9
Takenohata 1	0.96	88.2	11.8	0.0
Takenohata 2	0.73	64.3	30.9	4.9

n.a. = data are not available.

Table 1.
 Fuel loads in the grassland of Aso and fractions of the two major habitat plant species, *Miscanthus sinensis* and *Pleiblastus chino var. viridis*.

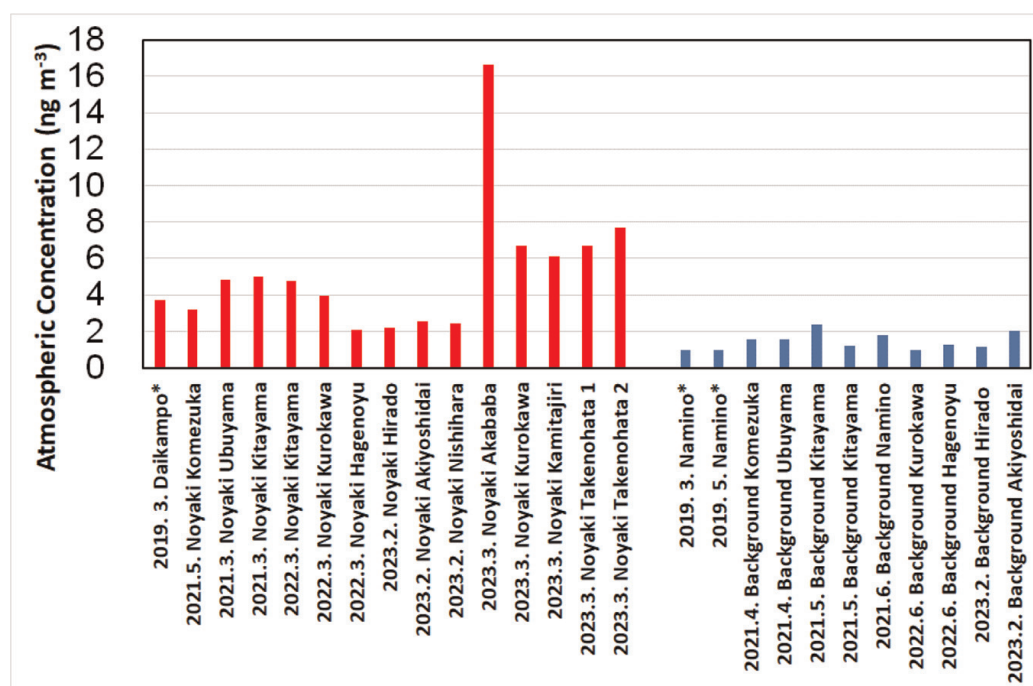
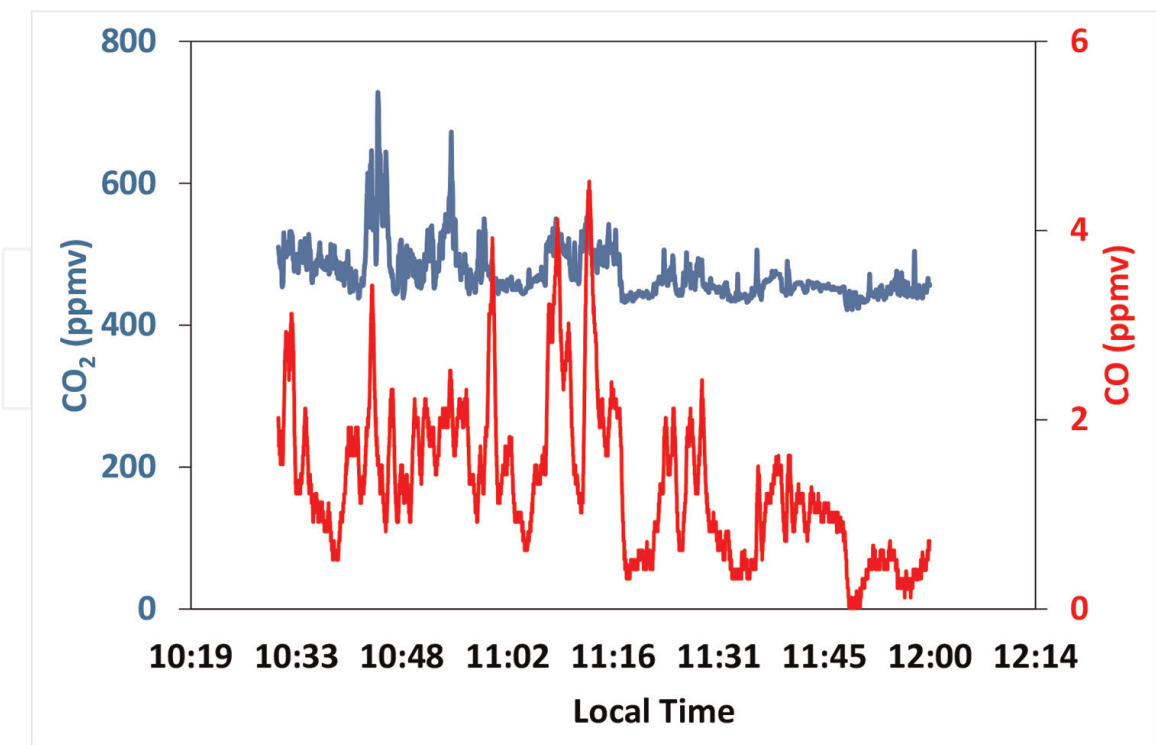
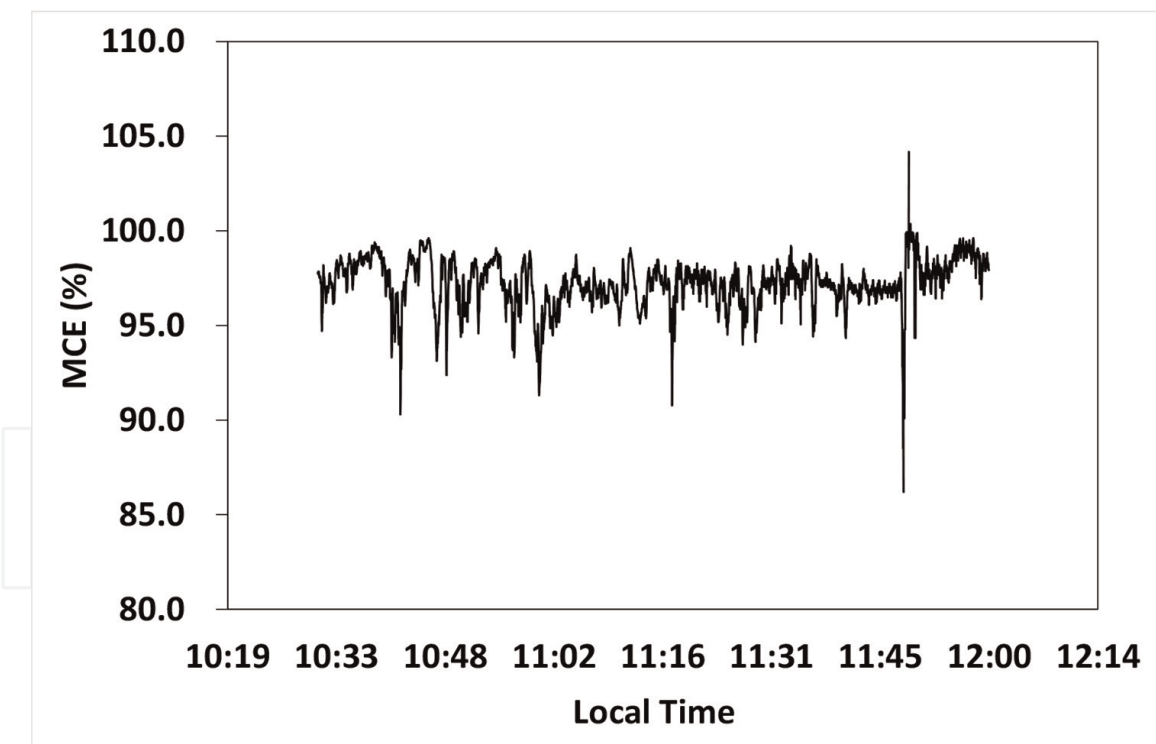


Figure 7.
 Average atmospheric concentrations of TGM observed during the Noyaki (red bar) and ordinary days (blue bar) in the period of 2019–2023.

The ground-based measurements of CO and CO₂ showed the complexity of the combustion state, flaming and smoldering. For example, observations for CO and CO₂ at Akiyoshidai in the time period between 10 AM and 12 PM demonstrated their unsynchronized variations in detail, but roughly speaking, their trends were similar (Figure 8a). MCEs in this time period varied from 86 to 104% and on average \pm SD, $97.2 \pm 1.3\%$ (Figure 8b). The fractions of CO relative to the sum of CO and CO₂ were on average \pm SD, $2.9 \pm 4.0\%$. The scatter plot of Δ CO against Δ CO₂ showed a high correlation ($r^2 = 0.768$) with a slope of 0.02, indicating a proportional relationship and nearly complete combustion (Figure 9).



(a)



(b)

Figure 8. Time series plot of (a) volume-based CO₂ (blue) and CO (red) mixing ratios, and (b) modified combustion efficiency (i.e., $\Delta\text{CO}_2/(\Delta\text{CO} + \Delta\text{CO}_2)$) observed during the prescribed grassland burning at the Akiyoshidai National Park.

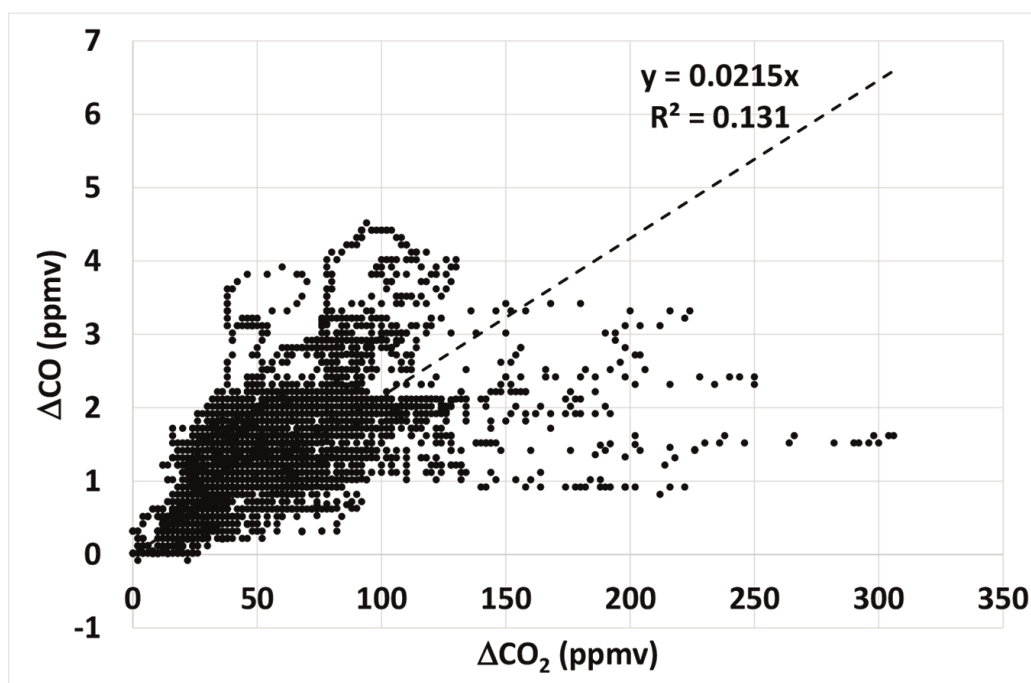


Figure 9. Scatter plot of excess CO and CO₂ mixing ratios (ΔCO and ΔCO_2) observed during the prescribed grassland burning at the Akiyoshidai National Park.

3.2.4 Excess concentration ratio, emission factor, and Total mercury emission

ERs for $\Delta\text{TGM}/(\Delta\text{CO}_2 + \Delta\text{CO})$ and $\Delta\text{TGM}/\Delta\text{CO}$ are approximately 1.6×10^{-9} and 0.56×10^{-7} , respectively. According to Eq. (2) with the assumptions that the carbon content of fuel was 50%, the majority of this carbon was converted to CO₂ and CO, and CO₂:CO was 0.97:0.03 (discussed in subsection 3.2.3 for MCE), the corresponding EFs estimated from the ERs for $\Delta\text{TGM}/(\Delta\text{CO}_2 + \Delta\text{CO})$ and $\Delta\text{TGM}/\Delta\text{CO}$ shown above are 13.2×10^{-6} and 14.0×10^{-6} g Hg kg⁻¹, respectively. The values are significantly low, compared to other EFs reported for the grassland fires ranging from 38 to 510×10^{-6} g Hg kg⁻¹ ([51], references therein). The results were obtained during the emission study in Akiyoshidai, therefore, we applied these EFs to the prescribed fire there. Given the FL of 1.0 kg m⁻² with the 11.4 km² of burned area reported [96]. The estimated Hg emission from there is 150.5 and 159.6 g y⁻¹, which is approximately 0.02% of the annual Japanese domestic emission of TGM that the Ministry of Environment Japan reported.

3.2.5 Stable mercury isotope ratios

A limited number of TGM samples collected using BAuTs were analyzed for stable mercury isotope ratios. In order to characterize the isotopic compositions we evaluated if the observed isotopic compositions were reflected by mass dependent fractionation (MDF) or mass independent fractionation (MIF) using the Eq. (4) [97].

$$\Delta^x\text{Hg}(\text{‰}) \approx \delta^x\text{Hg} - (\delta^{202}\text{Hg} \times \beta_x) \quad (4)$$

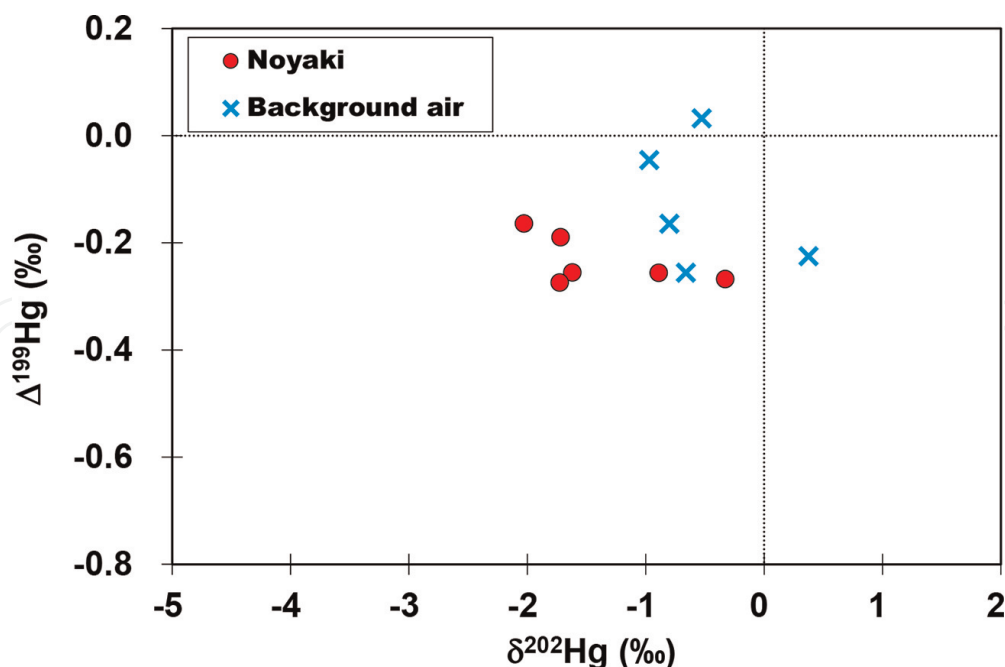


Figure 10.

Stable isotope ratios of TGM collected from the Noyaki plume and background air. The figure was reproduced from the previously published data [60]. See the text and Eqs. (3) and (4) for the definitions of these isotope ratios.

where β_x is the mass-dependent fractionation factor for mass x (0.2520, 0.5024, 0.7520, and 1.4930 for mass 199, 200, 201, and 204, respectively).

Results showed that $\Delta^{199}\text{Hg}$ values for TGM in the Noyaki plumes were on average (\pm SD), $-0.23 \pm 0.05\text{‰}$, while those for TGM in the background air were on average, $-0.13 \pm 0.12\text{‰}$, indicating TGM emitted from the Noyaki underwent small MIF and TGM in the background air did not. Furthermore, $\delta^{202}\text{Hg}$ of TGM from the background air and Noyaki plumes showed discrete compositions (**Figure 10**). It is interesting that our observations shown in **Figure 10** resembled the isotopic compositions found in plants, such as rice straw [75], foliage [79–81], and in soil [82]. Was atmospheric GEM aspirated from the air together with CO_2 , then oxidized and fixed in the plant body? Or was the deposited mercury on the ground taken up through the roots of plants? Answers to those open questions will be found by continuing overall grassland studies, including prescribed biomass burning and wet and dry deposition of mercury as well as mercury content in plant sections and soil.

4. Conclusion

Our study concretely confirmed that the prescribed biomass burning of the grasslands in Aso and other grasslands in western Japan emitted TGM into the atmosphere. The estimation of the emitted TGM during the Noyaki in the Aso region is currently under evaluation. Preliminary estimation of the TGM emission from Noyaki in the Akiyoshidai National Park resulted in 150–160 g TGM emission, which accounts for 0.02% of the whole domestic emission of mercury that the Japanese Ministry of Environment reported. Due to more than 10 times larger area of the Aso grassland than the Akiyoshi-dai grassland, it is possible that the emission of mercury from Noyaki in Aso can rise to 1% or similar, and for whole Noyaki in Japan may rise to a few %. The investigation is currently on-going.

$\delta^{199}\text{Hg}$ values of TGM showed similar values to the reported $\delta^{199}\text{Hg}$ of the plant uptake TGM, implying the atmospheric mercury can be the origin. However, our current dataset could not identify whether or not the plant uptake of TGM from the air or wet and/or dry depositions contributed to the grassland mercury. Further detailed study combined with atmospheric monitoring in the grassland may help us to find the answer.

Acknowledgements

The authors thank The Sumitomo Foundation (Grant number 2230266) and the National Institute for Minamata Disease (NIMD) for the financial support of the research on mercury emissions from the grassland burning. The authors also thank the assistant Nanami Yamamoto from the NIMD for assisting our laboratory work in this project.

Conflict of interest

The authors declare no conflict of interest.

Author details

Satoshi Irei^{1*}, Satoshi Kameyama², Hiroto Shimazaki³, Asahi Sakuma³ and Seiichiro Yonemura⁴

1 Department of Environment and Public Health, National Institute for Minamata Disease, Kumamoto, Japan


2 Biodiversity Division, National Institute for Environmental Studies, Ibaraki, Japan

3 Department of Civil Engineering, National Institute of Technology, Kisarazu College, Chiba, Japan

4 Faculty of Bioresource Sciences, Prefectural University of Hiroshima, Hiroshima, Japan

*Address all correspondence to: satoshireinimd@gmail.com

IntechOpen

© 2023 The Author(s). Licensee IntechOpen. This chapter is distributed under the terms of the Creative Commons Attribution License (<http://creativecommons.org/licenses/by/3.0>), which permits unrestricted use, distribution, and reproduction in any medium, provided the original work is properly cited. 

References

- [1] Geospatial Information Authority of Japan. Provision of Maps Clearly Showing Territory of Japan [Internet]. Available from: https://www.cas.go.jp/jp/ryodo_eg/torikumi/giaj.html [Accessed: September 7, 2023]
- [2] Statistics Bureau of Japan. Current Population Estimates as of October 1, 2022 [Internet]. Available from: <https://www.stat.go.jp/english/data/jinsui/2022np/index.html> [Accessed: September 7, 2023]
- [3] Ministry of Environment, Japan. White Paper; Annual Report on the Environment, the Sound Material-Cycle Society and Biodiversity in Japan. 2022
- [4] National Agriculture and Food Research Organization. Available from: https://www.naro.go.jp/project/results/lab/oratory/nilgs/2012/420b0_05_08.html
- [5] Ministry of Environment Kyushu Regional Environment Office, 2003, The Handbook of the Grassland of Aso (in Japanese). Revised March, 2007
- [6] Kumamoto Prefecture. Kumamoto Prefecture Tourism Statistics 2018 (in Japanese) [Internet]. 2020. Available from: https://www.pref.kumamoto.jp/uploaded/life/6411_126374_misc.pdf [Accessed: September 7, 2023]
- [7] Kumamoto Prefecture. Kumamoto Prefecture Tourism Statistics 2021 (in Japanese) [Internet]. 2022. Available from: <https://kumamoto.guide/files/af7bd824-5c2d-4038-bd89-4284c2525321.pdf> [Accessed: September 7, 2023]
- [8] Sasaki A, Sasaki N. Chapter 8: The history of grassland and human activity in the Aso Kuju region from the perspective of phytolith, pollen, and fine particulate carbon (in Japanese). In: Sato H, Kenji I, editors. The Environmental History of Wildland. Vol. 2, the Series 35000 Years of – Environmental History of Human and Nature. Tokyo: Bunichisogou shuppan; 2011. pp. 169-182. ISBN 978-4-8299-1196-9
- [9] Toda Y, Vegetation and Landscape of Aso. Special feature: The natural environment and landscape of Kyushu. Journal of Landscape Architecture. 1994; 57(4):338-345. (In Japanese)
- [10] Aso-Kuju National Park. Available from: <https://www.env.go.jp/park/aso/>
- [11] Aso Grassland Regeneration Executive Office. Chapter 2: Characteristics of Aso Grassland (in Japanese). In: The 3rd Aso Grassland Regeneration Plan [Internet]. 2021. Available from: https://www.aso-sougen.com/learn/files/mgz_03.pdf [Accessed: 2023]
- [12] Aso Pedia. Plants of Aso (in Japanese) [Internet]. 2015. Available from: <http://www.aso-dm.net/?%E9%98%BF%E8%98%87%E3%81%AE%E6%A4%8D%E7%89%A9> [Accessed: July 14, 2023]
- [13] Aso Geopark Promotion Council. Flora and Fauna of Aso (in Japanese). In: Aso Geopark Guidebook [Internet]. 2012. pp. 24-30. Available from: <http://www.aso-geopark.jp/mainsites/mainsite08.html> [Accessed: July 14, 2023]
- [14] Crutzen PJ, Heidt LE, Kransnec JP, Pollock WH, Seiler W. Biomass burning as a source of atmospheric trace gases CO, H₂, N₂O, NO, CH₃Cl, and COS. Nature. 1979;282(15):253-256

- [15] Hegg DA, Radke LF, Hobbs PV. Ammonia emissions from biomass burning. *Geophysical Research Letters*. 1988;**15**(4):335-337
- [16] Cofer WR III, Levine JS, Winstead EL, Stocks BJ. Gaseous emissions from Canadian boreal forest fires. *Atmospheric Environment*. 1990;**24A**(7):1653-1659
- [17] Cofer WR III, Levine JS, Winstead EL, Lebel PJ, Koller AM, Hinkle CR. Trace gas emissions from burning Florida wetlands. *Journal of Geophysical Research*. 1990;**95**(D2):1865-1870
- [18] Yokelson RJ, Goode JG, Ward DE, Susott RA, Babbitt RE, Wade DD, et al. Emissions of formaldehyde, acetic acid, methanol, and other trace gases from biomass fires in North Carolina measured by airborne Fourier transform infrared spectroscopy. *Journal of Geophysical Research*. 1999;**104**(D23): 30109-30125
- [19] Yokelson RJ, Crouse JD, DeCarlo PF, Karl T, Urbanski S, Atlas E, et al. Emissions from biomass burning in the Yucatan. *Atmospheric Chemistry and Physics*. 2009;**9**:5785-5812
- [20] Burling IR, Yokelson RJ, Akagi SK, Urbanski SP, Wold CE, Griffith DWT, et al. Airborne and ground-based measurements of the trace gases and particles emitted by prescribed fires in the United States. *Atmospheric Chemistry and Physics*. 2011;**11**: 12197-12216
- [21] Akagi SK, Burling IR, Mendoza A, Johnson TJ, Cameron M, Griffith DWT, et al. Field measurements of trace gases emitted by prescribed fires in southern US pine forests using an open-path FTIR system. *Atmospheric Chemistry and Physics*. 2014;**14**:199-215
- [22] Andreae MO, Artaxo P, Beck V, Bela M, Freitas S, Gerbig C, et al. Carbon monoxide and related trace gases and aerosols over the Amazon Basin during the wet and dry seasons. *Atmospheric Chemistry and Physics*. 2012;**12**: 6041-6065
- [23] Hurst DF, Griffith DW, Carras JN, Williams DJ, Fraser PJ. Measurements of trace gases emitted by Australian savanna fires during the 1990 dry season. *Journal of Atmospheric Chemistry*. 1994;**18**:33-56
- [24] Hurst DF, Griffith DWT, Cook GD. Trace gas emissions from biomass burning in tropical Australian savannas. *Journal of Geophysical Research*. 1994;**99**(D8):16441-16456
- [25] Shea RW, Shea BW, Kauffman JB, Ward DE, Haskins CI, Scholes MC. Fuel biomass and combustion factors associated with fires in savanna ecosystems of South Africa and Zambia. *Journal of Geophysical Research*. 1996;**101**(D19):23551-23568
- [26] Ward DE, Hao WM, Susott RA, Babbitt RE, Shea RW, Kauffman JB, et al. Effect of fuel composition on combustion efficiency and emission factors for African savanna ecosystems. *Journal of Geophysical Research*. 1996;**101**(D19):23569-23576
- [27] Cofer WR, Levine JS, Winstead EL, Cahoon DR, Sebacher DI, Pinto JP, et al. Source compositions of trace gases released during African savanna fires. *Journal of Geophysical Research*. 1996;**101**(D19):23597-23602
- [28] Le Canut P, Andreae MO, Harris GW, Wienhold FG, Zenker T. Airborne studies of emissions from savanna fires in southern Africa 1. Aerosol Emissions Measured with a Laser Optical Particle Counter. 1996;**101**(D19):23615-23630

- [29] Andreae MO, Andreae TW, Annegarn H, Beer J, Cachier H, Le Canut P, et al. Airborne studies of aerosol emissions from savanna fires in southern Africa: 2. Aerosol chemical composition. *Journal of Geophysical Research*. 1998; **103**(D24):32119-32128
- [30] Echalar F, Gaudichet A, Cachier H, Artaxo P. Aerosol emissions by tropical forest and savanna biomass burning: Characteristic trace elements and fluxes. *Geophysical Research Letters*. 1995; **22**(22):3039-3042
- [31] Yamazaki D, Kajiwara H, Kirii M, Ohira S, Toda K. Direct determination of polycyclic aromatic hydrocarbons in PM_{2.5} by thermal desorption-GC/MS and analysis of their diurnal/seasonal variations and field burning in Kumamoto (in Japanese). *Bunseki Kagaku*. 2015; **64**(8):571-579
- [32] Yokelson RJ, Susott R, Ward DE, Reardon J, Griffith DW. Emissions from smoldering combustion of biomass measured by open-path Fourier transform infrared spectroscopy. *Journal of Geophysical Research [Atmosphere]*. 1997; **102**(D15):18865-18877
- [33] Yonemura S, Sudo S, Tsuruta H, Kawashima S. Relations between light hydrocarbon, carbon monoxide, and carbon dioxide concentrations in the plume from the combustion of plant material in a furnace. *Journal of Atmospheric Chemistry*. 2002; **43**:1-19
- [34] Yonemura S, Kawashima S. Concentrations of carbon gases and oxygen and their emission ratios from the combustion of rice hulls in a wind tunnel. *Atmospheric Environment*. 2007; **41**:1407-1416
- [35] Hayashi K, Ono K, Kajiura M, Sudo S, Yonemura S, Fushimi A, et al. Trace gas and particle emissions from open burning of three cereal crop residues: Increase in residue moistness enhances emissions of carbon monoxide, methane, and particulate organic carbon. *Atmospheric Environment*. 2014; **95**: 36-44
- [36] Burling IR, Yokelson RJ, Griffith DWT, Johnson TJ, Veres P, Roberts JM, et al. Laboratory measurements of trace gas emissions from biomass burning of fuel types from the southeastern and southwestern United States. *Atmospheric Chemistry and Physics*. 2010; **10**:11115-11130
- [37] Friedli HR, Radke LF, Lu JY, Banic CM, Leaitch WR, PacPherson JJ. Mercury emissions from burning of biomass from temperate north American forests: Laboratory and airborne measurements. *Atmospheric Environment*. 2003; **37**:253-267
- [38] Obrist D, Moosmuller H, Schurmann R, Chen LWA, Kreidenwies SM. Particulate-phase and gaseous elemental mercury emissions during biomass combustion: Controlling factors and correlation with particulate matter emissions. *Environmental Science and Technology*. 2008; **42**(3):721-727
- [39] Czapiewski KV, Czuba E, Huang L, Ernst D, Norman AL, Koppmann R, et al. Isotopic composition of non-methane hydrocarbons in emissions from biomass burning. *Journal of Atmospheric Chemistry*. 2002; **43**:45-60
- [40] Friedli HR, Radke LF, Lu JY. Mercury in smoke from biomass fires. *Geophysical Research Letters*. 2001; **28**(17):3223-3226
- [41] Barbosa PM, Stroppiana D, Gregoire JM, Miguel J, Pereira C. An assessment of vegetation fire in Africa (1981-1991): Burned areas, burned biomass, and atmospheric emissions. *Global*

- Biogeochemical Cycles. 1999;**13**(4): 933-950
- [42] Mouillot F, Narasimha A, Balkanski Y, Lamarque JF, Field CB. Global carbon emissions from biomass burning in the 20th century. *Geophysical Research Letters*. 2006;**33**:L01801
- [43] Wiedinmyer C, Quayle B, Geron C, Belote A, McKenzie D, Zhang X, et al. Estimating emissions from fires in North America for air quality modeling. *Atmospheric Environment*. 2006;**40**: 3419-3432
- [44] Ito A, Penner JE. Global estimates of biomass burning emissions based on satellite imagery for the year 2000. *Journal of Geophysical Research*. 2004; **109**:D14S05
- [45] Akagi SK, Yokelson RJ, Wiedinmyer C, Alvarado MJ, Reid JS, Karl T, et al. Emission factors for open and domestic biomass burning for use in atmospheric models. *Atmospheric Chemistry and Physics*. 2011;**11**:4039-4072
- [46] Andreae MO. Emissions of trace gases and aerosols from biomass burning – An updated assessment. *Atmospheric Chemistry and Physics*. 2019;**19**: 8523-8546
- [47] Andreae MO, Merlet P. Emission of trace gasses and aerosols from biomass burning. *Global Biogeochemical Cycles*. 2001;**15**(4):955-966
- [48] Koppmann R, von Czapiewski K, Reid JS. A review of biomass burning emissions, part I: Gaseous emissions of carbon monoxide, methane, volatile organic compounds, and nitrogen containing compounds. *Atmospheric Chemistry and Physics Discussion*. 2005; **5**:10455-10516
- [49] Chen J, Li C, Ristovski Z, Milic A, Gu Y, Islam MS, et al. A review of biomass burning: Emissions and impacts on air quality, health and climate in China. *Science of Total Environment*. 2017;**579**:1000-1034
- [50] Veiga MM, Meech JA, Oñante N. Mercury pollution from deforestation. *Nature*. 1994;**368**:816-817
- [51] Wiedinmyer C, Friedli H. Mercury emission estimates from fires: An initial inventory for the United States. *Environmental Science and Technology*. 2007;**41**:8092-8098
- [52] Biswas A, Blum JD, Klaue B, Keeler GJ. Release of mercury from Rocky Mountain forest fires. *Global Biogeochemical Cycles*. 2007;**21**:GB1002
- [53] Engle MA, Gustin MS, Johnson DW, Murphy JF, Miller WW, Walker RF, et al. Mercury distribution in two Sierran forest and one desert sagebush steppe ecosystems and the effects of fire. *Science of Total Environment*. 2006;**367**: 222-233
- [54] Brunke E-G, Labuschagne C. Gaseous mercury emissions from a fire in the cape peninsula, South Africa, during January 2000. *Geophysical Research Letters*. 2001;**28**(8):1483-1486
- [55] Cinnirella S, Pirrone N. Spatial and temporal distributions of mercury emissions from forest fires in Mediterranean region and Russian federation. *Atmospheric Environment*. 2006;**40**:7346-7361
- [56] Albernaz P, Michelazzo M, Fostier AH, Magarelli G, Santos JC, de Carvalho Jr. A. Mercury emissions from forest burning in southern Amazon. *Geophysical Research Letters*. 2010;**37**: L09809
- [57] Sigler JM, Lee X, Munger W. Emission and long-range transport of

gaseous mercury from a large-scale Canadian boreal forest fire. *Environmental Science and Technology*. 2003;**37**:4343-4347

[58] Weiss-Penzias P, Jaffe D, Swartzendruber P, Hafner W, Chand D, Prestbo E. Quantifying Asian and biomass burning sources of mercury using the Hg/CO ratio in pollution plumes observed at the mount bachelor observatory. *Atmospheric Environment*. 2007;**41**:4366-4379

[59] Ebinghaus R, Slemr F, Brenninkmeijer CAM, van Velthoven P, Zahn A, Hermann M, et al. Emissions of gaseous mercury from biomass burning in South America in 2005 observed during CARIBIC flights. *Geophysical Research Letters*. 2007;**34**:L08813

[60] Friedli HR, Arellino FA, Cinnirella S Jr, Pirrone N. Chapter 8: Mercury emissions from global biomass burning: Spatial and temporal distribution. In: Pirrone N, Mason R, editors. *Mercury Fate and Transport in the Global Atmosphere: Measurements, Models and Policy Implications*. Interim Report of the UNEP Global Mercury Partnership Mercury Air Transport and Fate Research partnership area July 14. 2008. pp. 145-167

[61] Irei S. Isotopic characterization of gaseous mercury and particulate water-soluble organic carbon emitted from open grass field burning in Aso, Japan. *Applied Sciences*. 2022;**12**:109

[62] Irei S. Development of fast sampling and high recovery extraction method for stable isotope measurement of gaseous mercury. *Applied Sciences*. 2020;**10**:6691

[63] Du SH, Fang SC. Uptake of elemental mercury vapor by C3 and C4 species. *Environmental and Experimental Botany*. 1982;**22**(4):437-443

[64] Browne CL, Fang SC. Differential uptake of mercury vapor by Gramineous C3 and C4 plants. *Plant Physiology*. 1983;**72**:1040-1042

[65] Du SH, Fang SC. Catalase activity of C3 and C4 species and its relationship to mercury vapor uptake. *Environmental and Experimental Botany*. 1983;**23**(4): 347-353

[66] Hanson PJ, Lindberg SE, Tabberer TA, Owens JG, Kim K-H. Foliar exchange of mercury vapor: Evidence for compensation point. *Water, Air, and Solid Pollution*. 1995;**80**:373-382

[67] Lindberg SE. Forests and the global biogeochemical cycle of mercury: The importance of understanding air/vegetation exchange processes. In: Baeyens W, editor. *Global and Regional Mercury Cycles: Sources, Fluxes, and Mass Balances*. 1996. pp. 359-380

[68] Louis VLST, Rudd JWM, Kelly CA, Hall BD, Rolfhus KR, Scott KJ, et al. Importance of the forest canopy to fluxes of methyl mercury and total mercury to boreal ecosystems. *Environmental Science and Technology*. 2001;**35**:3089-3098

[69] Rea AW, Lindberg SE, Scherbatskoy T, Keeler GJ. Mercury accumulation in foliage over time in two northern mixed-hardwood forests. *Water, Air, and Soil Pollution*. 2002;**133**:49-67

[70] Ericksen JA, Gustin MS, Schorran DE, Johnson DW, Lindberg SE, Coleman JS. Accumulation of atmospheric mercury in forest foliage. *Atmospheric Environment*. 2003;**37**:1613-1622

[71] Millhollen AG, Gustin MS, Obrist D. Foliar mercury accumulation and exchange for three tree species. *Environmental Science and Technology*. 2006;**40**:6001-6006

- [72] Fay L, Gustin M. Assessing the influence of different atmospheric and soil mercury concentrations on foliar mercury concentrations in a controlled environment. *Water, Air, and Soil Pollution*. 2007;**181**:373-384
- [73] Friedli HR, Radke LF, Payne NJ, McRae DJ, Lynbam TJ, Blake TW. Mercury in vegetation and organic soil at an upland boreal forest site in prince albert national park. Saskatchewan. *Journal of Geophysical Research*. 2007; **112**:G01004
- [74] Obrist D, Johnson DW, Edmons RL. Effects of vegetation type on mercury concentrations and pools in two adjacent coniferous and deciduous forests. *Journal of Plant Nutrition and Soil Science*. 2012; **175**:68-77
- [75] Yin R, Feng X, Meng B. Stable mercury isotope variation in rice plants (*Oryza sativa* L.) from the Wanshan mercury mining district, SW China. *Environmental Science and Technology*. 2023;**47**:2238-2245
- [76] Fu X, Zhu W, Zhang H, Sommar J, Yu B, Yang X, et al. Depletion of atmospheric gaseous elemental mercury by plant uptake at Mt. Changbai, Northeast China. *Atmospheric Chemistry and Physics*. 2016;**16**:12861-12873
- [77] Jiskra M, Sonke JE, Obrist D, Bieser J, Edinghaus R, Myhre CL, et al. A vegetation control on seasonal variations in global atmospheric mercury concentrations. *Nature Geoscience*. 2018;**11**:244-250
- [78] Zhou J, Obrist D, Dastoor A, Jiskra M, Ryjkov A. Vegetation uptake of mercury and impacts on global cycling. *Nature Reviews*. 2021;**2**:269-284
- [79] Demers JD, Blum JD, Zak DR. Mercury isotopes in a forested ecosystem: Implications for air-surface exchange dynamics and the global mercury cycle. *Global Biogeochemical Cycles*. 2013;**27**:222-238
- [80] Yu B, Fu X, Yin R, Zhang H, Wang X, Lin CJ, et al. Isotopic compositions of atmospheric mercury in China: New evidence for sources and transformation processes in air and in vegetation. *Environmental Science and Technology*. 2016;**50**:9262-9269
- [81] Zheng W, Obrist D, Weis D, Bergquist BA. Mercury isotope compositions across north American forests. *Global Biogeochemical Cycles*. 2016;**30**:1475-1492
- [82] Jiskra M, Wiederhold JG, Skyllberg U, Kronberg RM, Hajdas I, Kretzschmar R. Mercury deposition and re-emission pathways in boreal forest soils investigated with Hg isotope signatures. *Environmental Science and Technology*. 2015;**49**:7188-7196
- [83] Meng B, Li Y, Cui W, Jiang P, Liu G, Wang Y, et al. Tracing the uptake, transport, and fate of mercury in sawgrass (*Cladima jamaicense*) in the Florida everglades using multi-isotope technique. *Environmental Science and Technology*. 2018;**52**(6):3384-3391
- [84] Ministry of Environment, Japan. Japan's Mercury Emission Inventory (FY 2020) [Internet]. 2023. Available from: <https://www.env.go.jp/content/000145228.pdf> [Accessed: September 6, 2023]
- [85] Cinnirella S, Pirrone N, Allegrini A, Guglietta D. Modeling mercury emissions from forest fires in the Mediterranean region. *Environmental Fluid Mechanics*. 2008;**8**:129-145
- [86] Payra S, Sharma A, Verma S. Chapter 14: Application of remote

sensing to study forest fires. In: Singh AK, Tiwari S, editors. *Atmospheric Remote Sensing Principles and Applications*. 2022. pp. 239-260

[87] Kurmaz B, Baylk C, Abdikan S. Forest Fire Area Detection by Using Landsat-8 and Sentinel-2 Satellite Images: A Case Study in Mugla, Turkey. 2020. Available from: <https://www.semanticscholar.org/paper/Forest-Fire-Area-Detection-by-Using-Landsat-8-and-A-Kurnaz-Bay%20C4%B1k/655389305d5975f58ea07f2c0ed64121c13ca86b> [Accessed: 2023]

[88] Hawbaker TJ, Vanderhoof MK, Schmidt GL, Beal Y-J, Picotte JJ, Takacs JD, et al. The Landsat burned area algorithm and products for the conterminous United States. *Remote Sensing of Environment*. 2020;**244**: 111801

[89] Ying L, Shen Z, Yang M, Piao S. Wildfire detection probability of MODIS fire products under the constraint of environmental factors: A study based on confirmed ground wildfire records. *Remote Sensing*. 2019;**11**(24):3031

[90] Ward DE, Radke LF. Chapter 4: Emissions measurements from vegetation fires: A comparative evaluation of methods and results. In: Crutzen PJ, Goldammer JG, editors. *The Ecological, Atmospheric, and Climatic Importance of Vegetation Fires*. City: John Wiley & Sons Ltd.; 1993. pp. 53-76. ISBN 0-471-93604-9

[91] Kumamoto Prefecture. Basic Research for Aso Grassland Regeneration Plan [Internet]. 2022. Available from: https://www.pref.kumamoto.jp/uploaded/life/181104_443400_misc.pdf [Accessed: 2023]

[92] Fu X, Heimbürger L-E, Sonke JE. Collection of atmospheric gaseous

mercury for stable isotope analysis using iodine- and chlorine-impregnated activated carbon traps. *Journal of Analytical Atomic Spectrometry*. 2014;**29**:841

[93] Yamakawa A, Takami A, Takeda Y, Kato S, Kajii Y. Emerging investigator series: Investigation of mercury emission sources using Hg isotopic compositions of atmospheric mercury at the Cape Hedo atmosphere and aerosol monitoring station (CHAAMS). *Japan. Environmental Science and Processing Impacts*. 2019;**21**:809-818

[94] Inomata H, Qong M, Suzuki Y, Fukuma M. Temporal variation of burned area of grassland in Aso – Analysis of landsat imagery (in Japanese). *Japanese Journal of Grassland Science*. 2006;**51**(4):341-347

[95] Bilbao B, Medina E. Types of grassland fires and nitrogen volatilization in tropical savannas of Calabozo, Venezuela. Chapter 55 in *Book Biomass Burning and Global Change Volume 2 Biomass Burning in South America, Southeast Asia, and Temperate and Boreal Ecosystems, and the Oil Fires of Kuwait*

[96] Ohta Y. Area of controlled burning of grassland on Akiyoshi-dai plateau. *Bulletin of the Akiyoshi-dai Museum of Natural History*. 2018;**53**:23-26. (in Japanese)

[97] Blum JD, Bergquist BA. Reporting of variations in the natural isotopic composition of mercury. *Analytical and Bioanalytical Chemistry*. 2007;**388**: 353-359